Combustion and Flame 157 (2010) 1540–1551

Contents lists available at ScienceDirect

Combustion and Flame

journal homepage: www.elsevier.com/locate/combustflame

Isobutane ignition delay time measurements at high pressure and detailed chemical kinetic simulations

D. Healy [a], N.S. Donato [b], C.J. Aul [b], E.L. Petersen [b], C.M. Zinner [c], G. Bourque [d], H.J. Curran [a,*]

[a] Combustion Chemistry Centre, School of Chemistry, NUI Galway, Ireland
[b] Department of Mechanical Engineering, Texas A&M University, College Station, TX, USA
[c] Mechanical, Materials and Aerospace Engineering, University of Central Florida, Orlando, FL, USA
[d] Rolls-Royce Canada Limited, 9500 Côte de Liesse, Lachine, Québec, Canada H8T 1A2

ARTICLE INFO

Article history:
Received 28 September 2009
Received in revised form 2 January 2010
Accepted 19 January 2010
Available online 17 February 2010

Keywords:
Isobutane
n-Butane
Oxidation
Modeling
Ignition delay
Shock-tube
Rapid compression machine

ABSTRACT

Rapid compression machine and shock-tube ignition experiments were performed for real fuel/air isobutane mixtures at equivalence ratios of 0.3, 0.5, 1, and 2. The wide range of experimental conditions included temperatures from 590 to 1567 K at pressures of approximately 1, 10, 20, and 30 atm. These data represent the most comprehensive set of experiments currently available for isobutane oxidation and further accentuate the complementary attributes of the two techniques toward high-pressure oxidation experiments over a wide range of temperatures. The experimental results were used to validate a detailed chemical kinetic model composed of 1328 reactions involving 230 species. This mechanism has been successfully used to simulate previously published ignition delay times as well. A thorough sensitivity analysis was performed to gain further insight to the chemical processes occurring at various conditions. Additionally, useful ignition delay time correlations were developed for temperatures greater than 1025 K. Comparisons are also made with available isobutane data from the literature, as well as with 100% *n*-butane and 50–50% *n*-butane–isobutane mixtures in air that were presented by the authors in recent studies. In general, the kinetic model shows excellent agreement with the data over the wide range of conditions of the present study.

1. Introduction

Butane and its isomers, while not ideal fuels for use on their own, play a significant role in the oxidation of larger hydrocarbons and are present in industrial fuels such as liquefied natural gas (LNG). In order to avoid combustion problems such as flashback, blow off, instabilities, and autoignition a complete understanding of fuel-blend chemistry is necessary at the conditions representative of engine applications [1–3]. It has also been shown that isobutane displays different ignition delay time behavior than that of *n*-butane [4], so a separate study of its oxidation behavior is warranted. The focus of this paper is therefore on the oxidation chemistry of isobutane, complementing companion papers on *n*-butane ignition [5] and a comparison of both isomers of butane [4]. The present work provides the validation of a comprehensive C_4 chemistry model at practical engine pressures and temperatures.

Although the ignition behavior of *n*-butane has been shown to differ from isobutane, only a few isobutane ignition studies have been performed [6–11]. Addagaria et al. [6] carried out experiments in a modified single cylinder research engine to study the correlation between heat release and engine knock. A skip-fire strategy was used to isolate the heat release due to chemical pre-ignition reactions. Pressure profiles of *n*- and isobutane mixtures indicated that there is a decrease in the heat release occurring during the second skip cycle, upon increasing the percentage of isobutane in the mixture.

Wilk et al. [7] used *n*- and isobutane in a test engine to examine the importance of molecular structure in determining knock tendency. The experimental results were interpreted using a detailed chemical kinetic model. Temporally resolved samples were withdrawn from the combustion chamber, providing measured histories of the concentration of a wide variety of reactants, olefins, carbonyl, and other intermediate and product species. Calculations showed that $R\dot{O}_2$ isomerization reactions are more important contributors to chain branching in the oxidation of *n*-butane relative to isobutane. Chain branching in isobutane was found to be dependent on H-atom abstraction reactions involving $H\dot{O}_2$ and $CH_3\dot{O}_2$ radicals that occur at higher temperatures than $R\dot{O}_2$ isomerization reactions.

Griffiths et al. [8] reported on the autoignition characteristics of isobutane, iso-octane, and toluene in addition to C_4–C_7 *n*-alkanes in stoichiometric mixtures with air following compression, to

* Corresponding author.
E-mail address: henry.curran@nuigalway.ie (H.J. Curran).
URL: http://c3.nuigalway.ie/ (H.J. Curran).

0010-2180/$ - see front matter © 2010 The Combustion Institute. Published by Elsevier Inc. All rights reserved.
doi:10.1016/j.combustflame.2010.01.011

temperatures in the range 600–950 K and pressures up to 9 bar. Emphasis was placed on the dependence of ignition delay on compressed gas temperature, on the evolution of reaction as portrayed in the pressure-time records and on features of light output associated with single- and two-stage ignition. They saw no evidence in the light output or pressure records for vigorous development of two-stage ignition during the oxidation of isobutane and iso-octane. The much lower reactivity of isobutane compared with that of *n*-butane was suggested to stem from its limited ability to undergo alkyl-peroxy radical isomerization and generate ȮH radicals via the low-temperature chain-branching process, due to higher strain energies involved in the isomerization reactions as a result of the tighter carbon atom structure.

Wang et al. [9] used a reduced chemical kinetic model to simulate the autoignition of the butane isomers from the non-fired test engine cycles under skip fired conditions. This model improved predictions of the heat release onset time and the magnitude of the heat release was well reproduced. Moreover, predictions of the fuel consumption and carbon monoxide formation were in reasonable agreement with the experimental data.

Oehlschlaeger et al. [10] measured ignition times and ȮH radical concentration time histories behind reflected shock waves during the oxidation of three branched alkanes: isobutane (2-methylpropane), iso-pentane (2-methylbutane), and iso-octane (2,2,4- trimethylpentane). Experiments behind reflected shock waves were recorded in the temperature range 1177–2009 K and 1.10–12.58 atm with dilute fuel/O_2/Ar mixtures varying in fuel concentration from 100 ppm to 1.25% and in equivalence ratio from 0.25 to 2. The ignition times and OH concentration time histories were compared to modeled predictions of seven branched alkane oxidation mechanisms available in the literature with varying results, which was to be expected as none of the models had been validated or optimized using transient radical pool data.

In another study published in the same year, Oehlschlaeger et al. [12] reported on the high-temperature thermal decomposition of *n*-butane and isobutane behind shock waves and measured the decomposition rates of both butane isomers in the falloff regime at high temperatures using UV narrow-line laser absorption of $\dot{C}H_3$ at 216.6 nm. An RRKM/master equation analysis with a restricted (hindered) Gorin model for the transition state was carried out and fit to the experimental data, resulting in pressure-dependent rate constants which were ultimately fit using the nine-parameter Troe formalism [13].

Ogura et al. [11] measured ignition delay times behind reflected shock waves for *n*-butane, isobutane and their mixtures at 1.0% fuel, at $\phi = 0.72$ diluted in argon at a pressure of approximately 2 atm. It was found that pure isobutane was slowest to ignite and *n*-butane the fastest, with ignition times in the order 100% *i*-C_4 > 70% *i*-C_4/30% *n*-C_4 > 50% *i*-C_4/50% *n*-C_4 > 30% *i*-C_4/70% *n*-C_4 > 100% *n*-C_4.

Most recently, the authors have published both experimental reflected-shock ignition delay times and kinetic modeling results for a 50% *n*-butane/50% isobutane blend over a wide range of stoichiometry ($\phi = 0.3$–2.0), temperature (1056–1598 K), and pressure (1–21 atm) [4]. The results of this work served as an initial validation for the chemical kinetic model described here.

In the current study, a new comprehensive set of ignition delay data over a wider range of equivalence ratio and pressure than ever previously reported for pure isobutane is presented. In addition, details of the chemical kinetic mechanism used to successfully simulate these new data are provided. Moreover, where possible we compare our data with those previously published in the literature. The present paper also serves as a companion to the paper on the ignition chemistry of *n*-butane [5]. Provided below is a brief overview of the experimental details, followed by a summary of the chemical kinetic model. The results of the study are presented next, including discussions of the trends, sensitivity analyses, and comparisons with archival data.

2. Experimental

Details of both the rapid compression machine (RCM) [14–16] and the shock tubes (ST) [17,18,20] have been provided previously, with a summary given in [19]. Details of the main mixture compositions are provided in Table 1. Some additional mixtures corresponding to compositions from the literature were also studied, the details of which are provided later in this paper.

For the RCM experiments, the isobutane was obtained from Aldrich at 99%+ purity, while all other gases were supplied by BOC Ireland; nitrogen (CP Grade) 99.95%, argon (Research Grade) 99.9995%, oxygen (Medical Grade) 99.5%, and all were used without further purification. Test mixtures were prepared manometrically in a stainless steel container and allowed to mix thoroughly before use. For the shock-tube experiments, the isobutane was obtained from Matheson at a Research Purity grade of 99.995%; the nitrogen and oxygen were purchased in a premixed bottle from Matheson at a volumetric ratio of 3.76, herein designated as "air", at a purity of 99.9995%. All mixtures in the shock-tube experiments were also prepared manometrically in mixing tanks utilizing jet-induced turbulence to ensure proper mixing [18,20].

A sample plot showing pressure and emission traces for a typical shock-tube experiment involving isobutane is provided as Fig. 1 in the supplemental material. All other experimental details, including the definition of ignition delay time, are provided in the companion paper on *n*-butane ignition [5].

3. Model

The mechanism is as described in the companion paper for *n*-butane [5], but four changes were made to the isobutane mechanism relative to *n*-butane in order to more accurately simulate these experimental results. We did not alter the *n*-butane rate constants as these are distinct differences. Moreover, in simulating the isobutane experiments, the same heat loss model as for *n*-butane [5] was applied.

3.1. Hydrogen abstraction by $H\dot{O}_2$ and $CH_3\dot{O}_2$

For abstraction by hydroperoxyl ($H\dot{O}_2$) and methylperoxyl ($CH_3\dot{O}_2$) radicals, the rate constants are as described in the companion paper [5]. However, in order to obtain better agreement with the model, the rate of abstraction of a tertiary hydrogen atom was decreased by 33% for both $H\dot{O}_2$ and $CH_3\dot{O}_2$ radicals. As these are the most important radicals consuming the fuel in the temperature range 850–1100 K, this decreased rate has the effect of decreasing the overall reactivity of the system, thus improving the mechanism agreement in this temperature range. Rate constants for abstraction by $H\dot{O}_2$ and $CH_3\dot{O}_2$ radicals are provided in Table 2.

Table 1
Main isobutane mixtures tested. Percentages are on a molar basis.

% *i*-C_4H_{10}	O_2	Diluent	ϕ
0.962	20.83	78.21	0.3
1.595	20.70	77.71	0.5
3.135	20.38	76.49	1.0
6.079	19.76	74.16	2.0

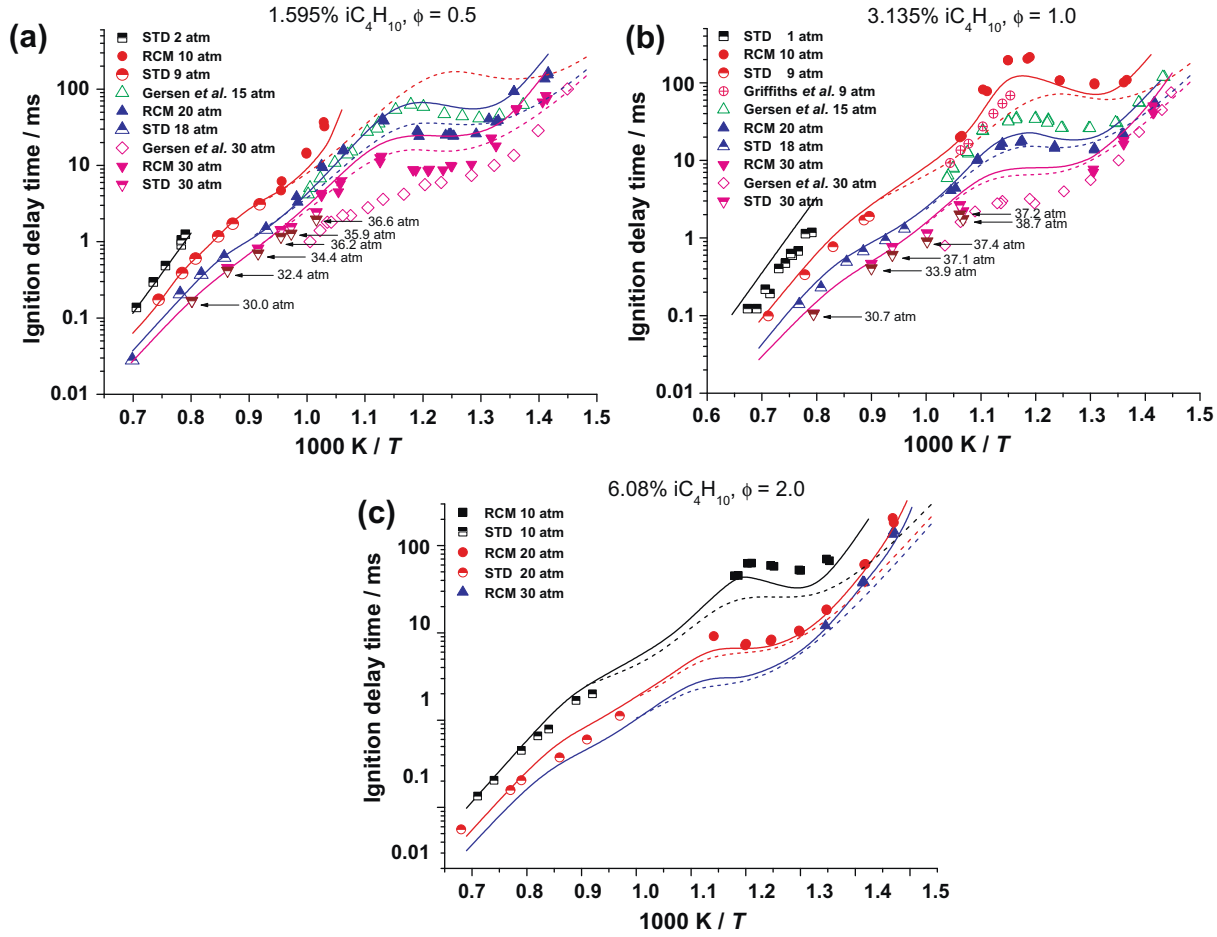

Fig. 1. Effect of pressure on ignition delay times from both the RCM and ST data sets for iso-C_4H_{10} oxidation in "air". Lines are model simulations, solid lines include heat losses, dashed lines assume adiabatic conditions. STD = shock-tube data.

Table 2
Arrhenius parameters per H-atom (cm^3 mol s cal units). Nomenclature applies to the modified Arrhenius rate coefficients k defined as $k = \mathscr{A}T^n \exp(\mathscr{E}_a/RT)$.

Abstraction by	C-type	$\mathscr{A}$	n	$\mathscr{E}_a$
HO_2	Primary	6.80×10^{00}	3.59	17,160
	Secondary	3.16×10^{01}	3.37	13,720
	Tertiary	4.33×10^{02}	3.01	12,090
CH_3O_2	Primary	2.31×10^{-01}	3.97	18,280
	Secondary	5.09×10^{00}	3.58	14,810
	Tertiary	1.37×10^{02}	3.12	13,190

3.2. Alkyl radical decomposition

The first-formed radicals, iso-butyl ($i\dot{C}_4H_9$) and *tert*-butyl ($t\dot{C}_4H_9$) can decompose primarily by β-scission.

$$i\dot{C}_4H_9 \overset{1057}{\rightarrow} iC_4H_8 + \dot{H}$$
$$i\dot{C}_4H_9 \overset{1058}{\rightarrow} C_3H_6 + \dot{C}H_3$$
$$t\dot{C}_4H_9 \overset{1059}{\rightarrow} iC_4H_8 + \dot{H}$$

Rate constants for these reactions are taken from the work of Curran [21].

3.3. Alkyl radical isomerization

Inter-isomerization of iso-butyl and *tert*-butyl radicals involves a 1,2 H-shift. This reaction has been included as per the work of Matheu et al. [22], with the reverse rate calculated using microscopic reversibility.

3.4. Direction elimination of olefin + $H\dot{O}_2$ from alkyl-peroxy radical

A rate constant of $2.265 \times 10^{35} T^{-7.22} \exp(-19{,}874/T)\ s^{-1}$ is employed for the reaction $iC_4H_9\dot{O}_2 = iC_4H_8 + H\dot{O}_2$, while for $tC_4H_9\ \dot{O}_2 = iC_4H_8 + H\dot{O}_2$ a rate constant of $7.61 \times 10^{42} T^{-9.41} \exp(-20{,}881/T)\ s^{-1}$ is estimated. The rate constant for $iC_4H_9\dot{O}_2 = iC_4H_8 + H\dot{O}_2$ is approximately three times slower than that calculated by DeSain et al. [23] for the elimination of propene and a hydroperoxyl radical from *n*-propylperoxy radical. The rate constant for the reaction $tC_4H_9\dot{O}_2 = iC_4H_8 + H\dot{O}_2$ is 25% lower than the calculation of DeSain et al. for elimination of propene and hydroperoxyl radical from iso-propylperoxy radical. These rate constants are crude estimates, and further calculations need to be performed to calculate these rates more accurately.

3.5. $\dot{O}_2$QOOH isomerization to carbonylhydroperoxide + $\dot{O}H$

Rate constants for reaction $iC_4H_8OOH - i\dot{O}_2 = iC_4ketii + \dot{O}H$ and for the reaction $iC_4H_8OOH - t\dot{O}_2 = iC_4ketit + \dot{O}H$ were increased by a factor of two relative to those indicated in our companion *n*-butane paper. It is necessary to increase these rate constants because, in the temperature range 650–950 K, the reactivity of all isobutane mixtures was extremely sensitive to these reactions. This change is addressed further in the discussion on sensitivity analysis below.

The rate constants used for both *n*-butane and isobutane are provided in the reaction mechanism available online.

4. Results and discussion

All ignition delay times measured in both the ST and in the RCM are provided in Tables 1–18 of the supplemental material. In measuring isobutane ignition delay times in the rapid compression machine, which includes the negative temperature coefficient (NTC) region, no experimental cool-flame pressure rise was observed. These findings are in agreement with those of Griffiths et al. [8] in their investigations into the cool flame chemistry of the butane isomers. The model too does not predict the onset of a cool flame, which agrees with the experimental observations.

4.1. Effect of pressure on ignition

Fig. 1a–c shows comparisons of experimental results and model predictions for various isobutane mixtures at equivalence ratios of 0.5, 1.0 and 2.0. Fig. 1a shows results for a 1.595% *iso*-C_4H_{10} mixture at $\phi = 0.5$ in "air" at pressures of approximately 2, 10, 20, and 30 atm in addition to data reported by Gersen et al. [24] in an RCM at 15 and 30 atm. Observe the complementary nature of the entire RCM/shock-tube study; the RCM data were recorded in the temperature range 670–1000 K approximately, while the shock-tube data extend the temperature range from 1000 to 1567 K. For several pressures and equivalence ratios, the ST and RCM meet at nearly coincident temperatures, with remarkable agreement between the two techniques. At 10 atm, the fuel does not react below approximately 950 K, while at 20 and 30 atm the fuel reacts at temperatures of 700 and 670 K, respectively, and exhibits NTC behavior in the temperature range 670–1000 K.

It is apparent that reactivity increases with increasing pressure, as a *decrease* in ignition delay time with an *increase* in pressure at constant temperature was observed. Furthermore, the effect of increasing pressure is most pronounced in the NTC region, over the temperature range 760–950 K. The Gersen data are faster than the NUI Galway data at 30 atm throughout the temperature range of this study, and our RCM data shows a distinct negative temperature coefficient behavior not observed in the work of Gersen et al. Moreover, this NTC behavior is predicted by the model, but predicted ignition delay times are substantially slower than those measured at 30 atm. There is overlap in the temperature range 870–1000 K between the 15 atm Gersen data and the 20 atm NUI Galway data. Shock-tube data at pressures near 30 atm appear to line up with the RCM data of the present study and the predictions of the mechanism.

The mechanism is in poor agreement with the experimental results for the higher-pressure conditions and at the lower temperatures of the RCM data. In the NTC region in particular (670–1000 K), the model is consistently more than a factor of two slower than the experimental results at 20 and 30 atm. We have also simulated all RCM data assuming adiabatic conditions, used to illustrate an extreme change in mechanism simulations, and these are included as dashed lines in Fig. 1a–c. It is evident that heat losses are most significant for the lean ($\phi = 0.5$) mixture, and at a compressed gas pressure of 10 atm, but heat loss becomes less important as the pressure increases to 20 and 30 atm, and as the equivalence ratio increases to stoichiometric and rich ($\phi = 2.0$) conditions, corresponding to increased fuel densities.

A similar comparison depicting the effect of pressure is shown for a 3.133% isobutane mixture at $\phi = 1.0$ in "air" at 1, 10, 15, 20, and 30 atm pressure, Fig. 1b. In this graph are also plotted the experimental RCM data of Griffiths et al. [8] reported at 9 atm, and Gersen et al. data at 15 and 30 atm. The present RCM data at 10 atm are slower than those of Griffiths et al. The data of Gersen et al. at 15 atm are intermediate to the 10- and 20-atm data of this study and the 9-atm data of Griffiths et al. At 30 atm, where overlap exists, the present data agree with those of Gersen et al. The model is faster compared to the data at 10 atm but is slightly slower than the results at 20 and 30 atm. Moreover, it is slightly slower compared with the higher-temperature shock-tube results at all pressures.

For the third grouping of RCM and ST data, Fig. 1c shows the effect of pressure for a 6.08% isobutane mixture at $\phi = 2.0$ in "air". Again, increasing pressure reduces ignition delay time and increases the reactivity of the system. The model is again faster compared to experiment at 10 atm, but is in reasonably good agreement with experimental results at both 20 and 30 atm. Nonetheless, the general conclusion that can be drawn from the results for the three different stoichiometries in Fig. 1 is that the agreement between the model and both data sets (RCM and ST) is overall excellent, particularly when considering the wide range of conditions covered in this study.

Shown in Fig. 2 are shock-tube data for the leanest equivalence ratio, $\phi = 0.3$, in comparison with the kinetic mechanism. Three pressure ranges are compared: 2, 8.5, and 18 atm. Again, there is overall excellent agreement between data and model, with the best agreement being at the higher pressures. Provided in the following section are comparisons focusing on the effect of equivalence ratio for the complete RCM-ST data set.

4.2. Effect of equivalence ratio on ignition

Fig. 3a–d illustrates the effect of equivalence ratio on ignition delay time. Fig. 3a shows data recorded for isobutane mixtures at equivalence ratios of 0.3, 0.5, 1.0, and 2.0 in "air" at pressures in the range 1–2 atm. At these low-pressure and relatively high-temperature conditions, fuel-lean mixtures are most reactive while fuel-rich mixtures are slowest to ignite at constant temperature. This is common to all alkane fuels at these conditions, where the rate of the dominant chain-branching reaction $\dot{H} + O_2 \rightarrow \ddot{O} + \dot{O}H$ depends on the concentration of molecular oxygen. In Fig. 3b–d, the dependence on equivalence ratio is reversed; at these lower-temperature, higher-pressure conditions, fuel-lean mixtures are slowest to ignite, with the fuel-rich mixtures fastest due to the main chain-branching reactions emanating from the fuel.

Fig. 3a also shows that there is excellent agreement between the model and experiment at $\phi = 0.3$ and 0.5, but for stoichiometric and fuel-rich mixtures ($\phi = 2.0$) the model over-predicts ignition delay times by approximately a factor of two.

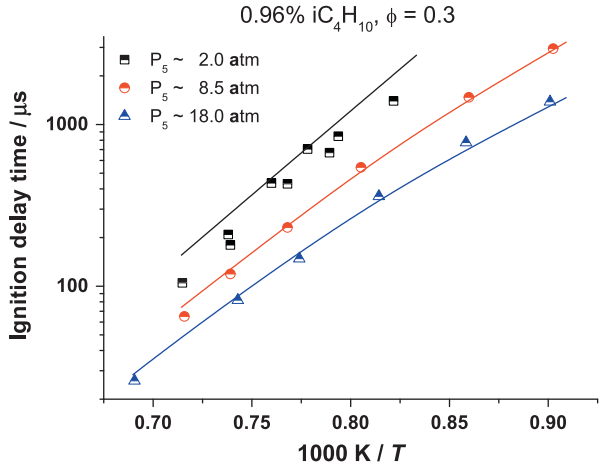

Fig. 2. Shock-tube data at an equivalence ratio of 0.3 in comparison with the model at three different pressures. Lines represent the model predictions.

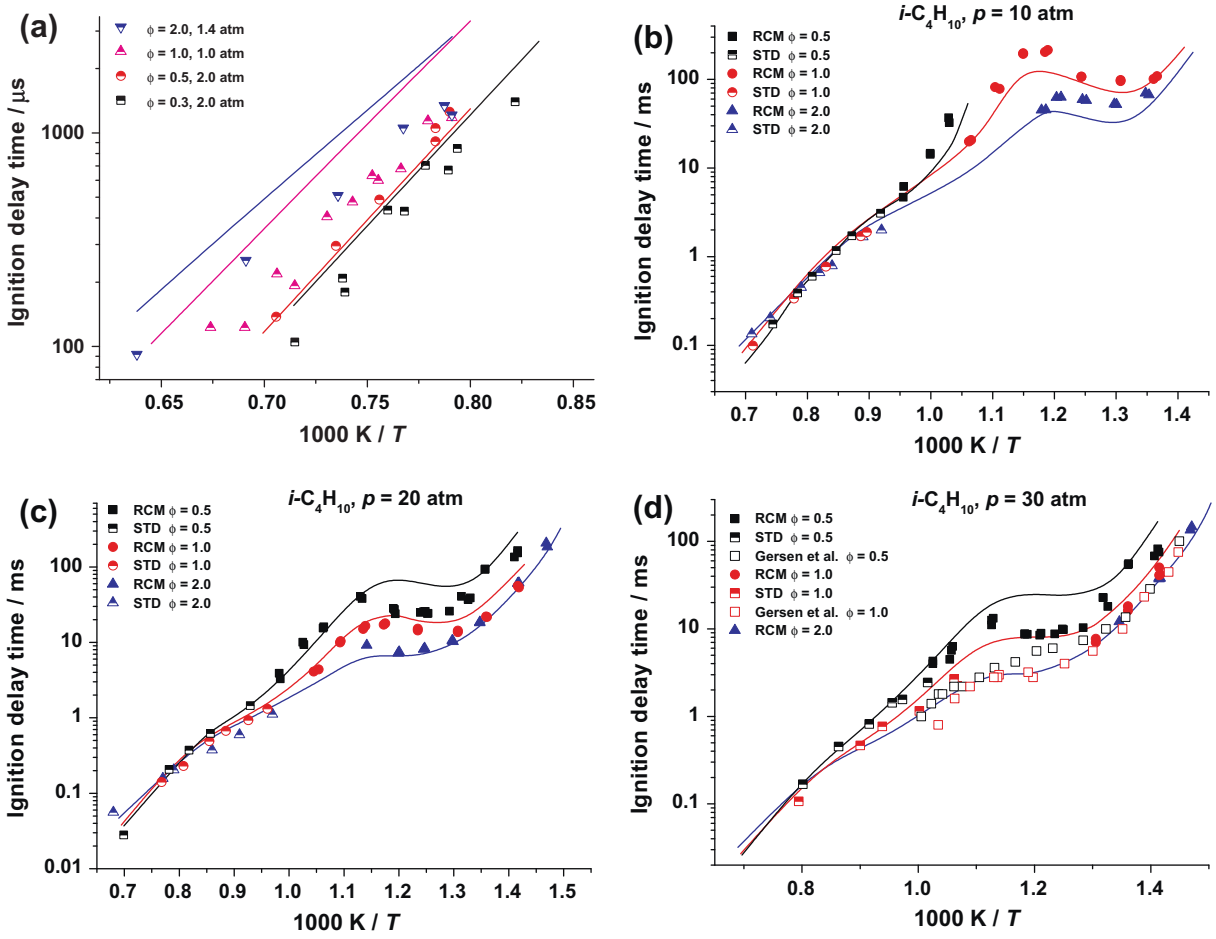

Fig. 3. Effect of equivalence ratio on ignition delay times for iso-C_4H_{10} oxidation in "air". Lines are model simulations.

Fig. 3b shows data recorded for isobutane mixtures in air at 10-atm pressure at equivalence ratios of 0.5, 1.0 and 2.0. At low temperatures (650–1100 K), lean mixtures are slowest to ignite, whereas rich mixtures are fastest. The greatest dependence on equivalence ratio occurs in the NTC region, in the temperature range 800–910 K. In the temperature range 1100–1250 K, there appears to be no dependence on equivalence ratio with all mixtures igniting at about the same time when at the same temperature and pressure. At temperatures above approximately 1250 K, high-temperature kinetics become prominent as the $\dot{H} + O_2$ chain-branching reaction dominates. The model captures this transition almost perfectly.

Fig. 3c shows data recorded for isobutane mixtures at 20-atm pressure. Again, the same trends as observed at 10 atm are seen, in that at low temperatures (650–1000 K) lean mixtures are slowest to ignite and rich mixtures are fastest. At 20 atm (Fig. 3c), there appears to be a lesser dependence of ignition delay time on equivalence ratio compared to that observed at 10 atm. This result is probably attributable to greater heat losses at 10 atm compared to 20 atm in the RCM. In this figure too is plotted the data recorded by Gersen et al. [24] at $\phi = 1.0$, albeit at an average compressed-gas pressure of 15 atm. Their data and those recorded in this study are in relatively good agreement. Moreover, there is overall excellent agreement between the mechanism and the data for these mixtures.

Finally, Fig. 3d shows data recorded for isobutane mixtures at 30-atm pressure. Again, the same trends are observed here as were observed at 10 and 20 atm, in that lean mixtures are slowest to ignite at low temperatures and rich mixtures are fastest. In this figure too is plotted the data recorded by Gersen et al. [24] at $\phi = 0.5$ and 1.0. At an equivalence ratio of 0.5, it is evident that the present data are consistently approximately a factor of two slower than those recorded by Gersen et al. and are in fact almost an order of magnitude slower than the Gersen data at 900 K. The model too predicts slightly lower reactivity than observed at $\phi = 0.5$ but is substantially slower than the data recorded by Gersen et al. for lean and stoichiometric conditions. For the ST data at 30 atm, the model has generally good agreement for both stoichiometries available ($\phi = 0.5$, 1.0).

4.3. Correlation results

Correlations describing the ignition delay time behavior of isobutane have been derived for the shock-tube conditions covering intermediate to high temperatures ($T > 1025$ K). The correlations were developed in the same manner as previously described by the present authors in the companion *n*-butane paper [5]. The basic form of the correlation is as follows:

$$\tau_{ign} = A[\mathrm{FUEL}]^x[\mathrm{AIR}]^y \exp(E/RT)$$

where τ_{ign} is the ignition delay time in μs; [FUEL] is the fuel concentration in mol/cm^3; [AIR] is the air concentration in mol/cm^3; and E, A, x, and y are constants. The constant E is commonly referred to as an ignition activation energy which is in kcal/mol, and R is the ideal gas constant in kcal/mol-K units. As in the *n*-butane study, intermediate- and high-temperature correlations were developed for 100%

isobutane. The following equation gives the correlation for the high-temperature ($1175 < T\,(\mathrm{K}) < 1567$) case.

$$\tau_{ign} = 6.616 \times 10^{-8}[i-\mathrm{C_4H_{10}}]^{0.06}[\mathrm{AIR}]^{-0.72}\exp(41.2/RT)$$

For the high-temperature 100% isobutane ignition delay times, a pressure dependence of $P^{-0.66}$ was found, which is slightly different from the pressure dependency of $P^{-0.54}$ found for high-temperature *n*-butane [5]. However, the activation energy of 41.2 kcal/mol for the isobutane correlation is very close to the *n*-butane result of 40.3 kcal/mol [5]. Fig. 4 shows good agreement between the high-temperature correlation and the experimental data in the left-side plot. At intermediate temperatures, a different ignition activation tends to correlate the data better, so a second correlation was determined for intermediate temperatures ($1025 < T\,(\mathrm{K}) < 1175$). This intermediate-temperature equation is given below.

$$\tau_{ign} = 4.872 \times 10^{-7}[i-\mathrm{C_4H_{10}}]^{-0.41}[\mathrm{AIR}]^{-0.69}\exp(23.1/RT)$$

Adding the exponents of the fuel and air terms yields a pressure dependence of $P^{-1.10}$. This pressure dependence is close to that found for *n*-butane (−1.04), but the activation energy of 23.1 kcal/mol for isobutane is about 5 kcal/mol lower than that found for *n*-butane (28.0 kcal/mol) [5]. Comparing the experimental data to the intermediate-temperature correlation, once again, reveals good agreement as shown in the right plot in Fig. 4.

The model was run over the conditions of the experimental range to determine predicted ignition delay times. The model results were then compared with the correlation. Fig. 4 shows excellent agreement between the predicted results and the correlation, as well as the experimental results for the same range of temperature, pressure and equivalence ratio. The activation energy, *E*, for the high-temperature correlation is larger than that of the intermediate-temperature correlation, as is also true for *n*-butane [5] and mixtures of 50/50 *n*-/*i*-butane [4]. This difference corresponds to a steeper slope when plotted against inverse temperature.

4.4. Reaction path and sensitivity analysis

A reaction pathway analysis was carried out for the RCM conditions outlined in Fig. 5, at 15% fuel conversion, at 10 atm and 875 K and at $\phi = 1.0$, which is an "average" experimental condition and lies in the middle of the NTC region. The reaction scheme shows that the fuel undergoes hydrogen-atom abstraction mainly by $\dot{\mathrm{O}}\mathrm{H}$ radicals, with a smaller contribution from $\mathrm{H\dot{O}_2}$ radicals and $\dot{\mathrm{H}}$ atoms, producing iso-butyl radicals, which accounts for 61% of the total fuel consumed, and *tert*-butyl radicals, which accounts for 39% of the fuel. The iso-butyl radical undergoes β-scission to form propene and a methyl radical (45% of the total flux) and/or adds to molecular oxygen to generate the iso-butylperoxy radical (15.9%). The *tert*-butyl radical adds to molecular oxygen forming a *tert*-butylperoxy radical. For both the iso- and *tert*-butylperoxy radicals, the main consumption route is via the molecular elimination channel to form isobutene and a hydroperoxyl radical. At this temperature, only a small amount of the fuel (4.5%) ends up as hydroperoxy-butyl radicals ($\mathrm{i\dot{C}_4H_8OOH-i}$). This radical is consumed via three pathways:

$$\mathrm{i\dot{C}_4H_8OOH-i} + O_2 \overset{16\%}{\rightarrow} \mathrm{iC_4H_8OOH-i\dot{O}_2}$$

$$\mathrm{i\dot{C}_4H_8OOH-i} \overset{29\%}{\rightarrow} \mathrm{cC_4H_8O} + \dot{\mathrm{O}}\mathrm{H}$$

$$\mathrm{i\dot{C}_4H_8OOH-i} \overset{54\%}{\rightarrow} \mathrm{C_3H_6} + \mathrm{CH_2O} + \dot{\mathrm{O}}\mathrm{H}$$

where $\mathrm{cC_4H_8O}$ is 3-methyl oxetane.

Isobutene mainly undergoes hydrogen abstraction reactions (35.9% of fuel flux) to form the methylallyl ($\mathrm{i\dot{C}_4H_7}$) radical which reacts mainly with $\mathrm{H\dot{O}_2}$ and $\mathrm{CH_3\dot{O}_2}$ radicals to form methyl-allyloxy ($\mathrm{iC_4H_7\dot{O}}$) radicals and hydroxyl and methoxyl radicals, respectively. A smaller fraction (7.6% of the fuel flux) of isobutene reacts with hydroperoxyl radicals to form 2,2-dimethyl oxirane ($\mathrm{iC_4H_8O}$) and a hydroxyl radical. Finally, hydroxyl radicals may also add to isobutene (8.1% of the fuel flux), and the radical formed then adds to molecular oxygen, undergoes an internal hydrogen atom isomerization, and decomposes via the Waddington mechanism [25,26].

A sensitivity analysis was performed to investigate the sensitivity of ignition delay time to various reactions in the isobutane submechanism as a function of temperature (Fig. 6) and equivalence ratio (Fig. 7). The analyses were performed by increasing and decreasing both the forward and reverse rate constants by a factor of two, with sensitivities expressed using the formula:

$$\ln S = \frac{\ln(\tau_+/\tau_-)/\ln(k_+/k_-)}{\ln(k_+/k_-)} = \frac{\ln(\tau_+/\tau_-)}{\ln(2/0.5)}$$

Fig. 6 depicts sensitivity coefficients for a stoichiometric isobutane/air mixture at 830, 950, 1200, and 1500 K and at a pressure of 20 atm. Sensitivity coefficients under lean and rich conditions are also provided in Figs. 2 and 3 of the supplemental material, but for

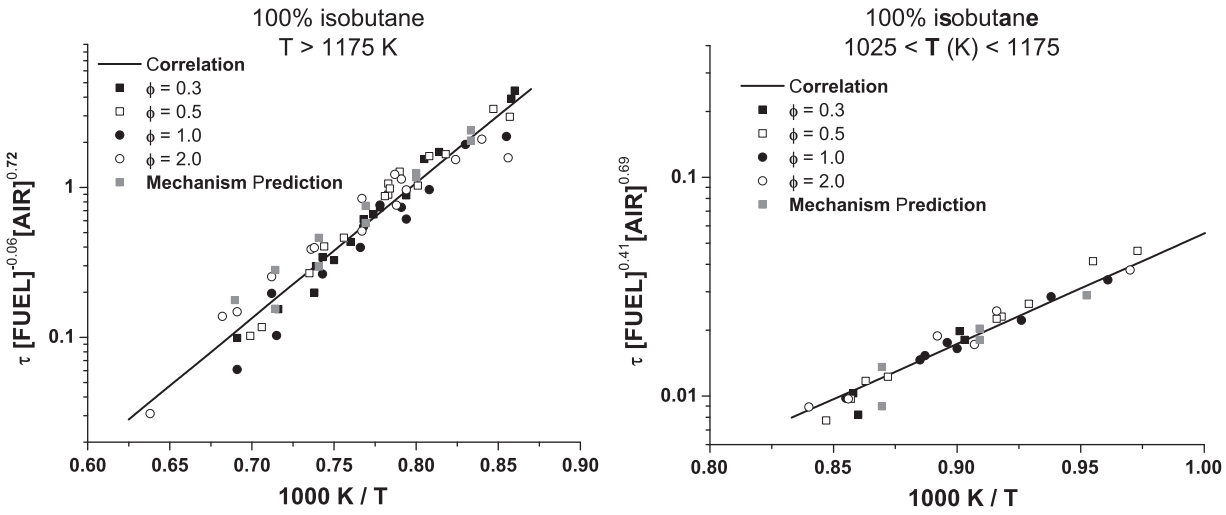

Fig. 4. High-temperature ($1175 < T\,(\mathrm{K}) < 1567$) correlation (left) and intermediate-temperature correlation ($1025 < T\,(\mathrm{K}) < 1175$) (right) in comparison to the experimental data and the results of the model. τ_{ign} in μs, [FUEL] and [AIR] in mol/cm^3.

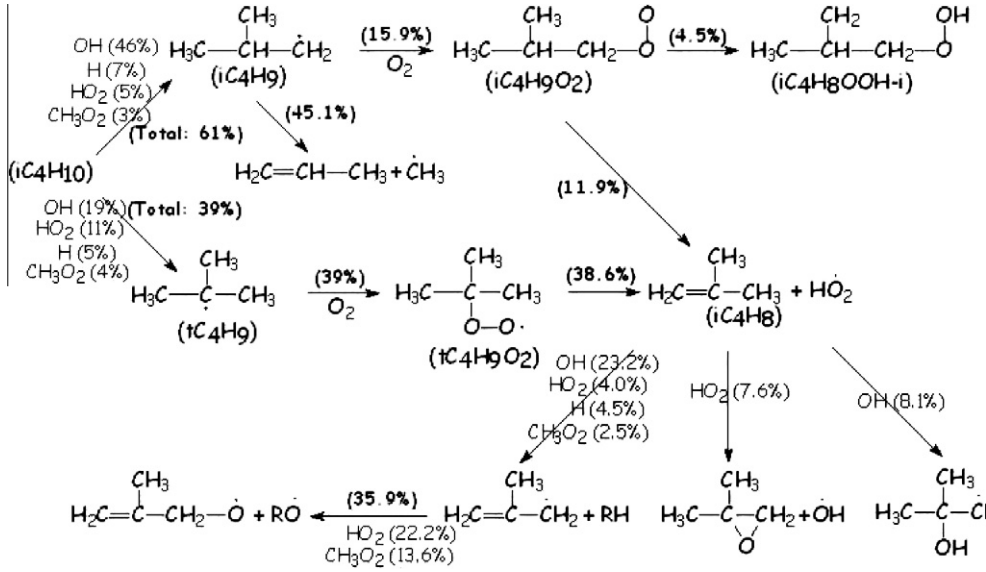

Fig. 5. Reaction path analysis for isobutane in a RCM for the NTC region; ϕ = 1, 875 K, 10 atm, 15% fuel consumed.

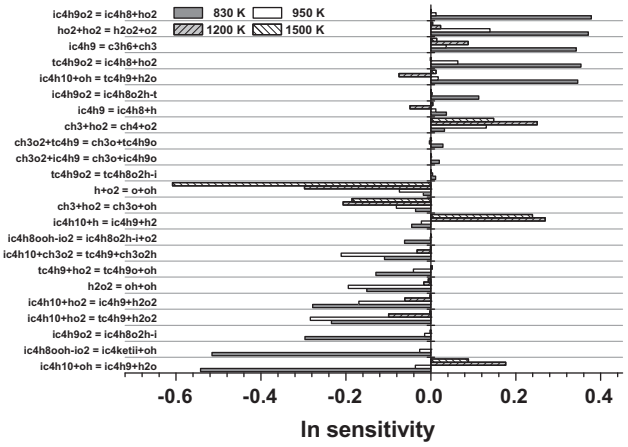

Fig. 6. Sensitivity coefficients showing the effect of temperature on isobutane ignition time, ϕ = 1.0, p = 20 bar.

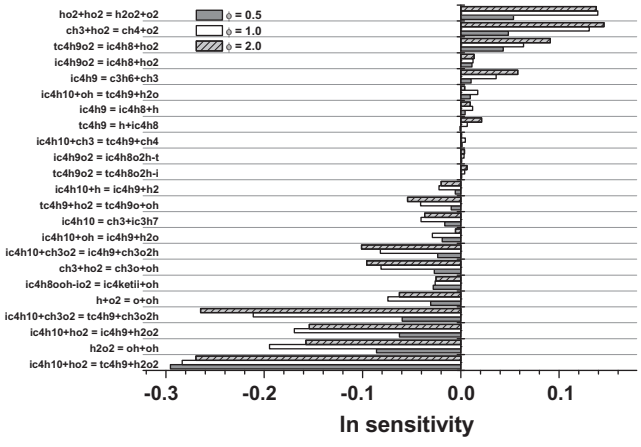

Fig. 7. Sensitivity coefficients showing the effect of equivalence ratio on isobutane ignition time, T = 950 K, p = 20 bar.

all equivalence ratios, the sensitivities are similar. A positive sensitivity indicates an increase in the ignition time and thus a *decrease* in overall reactivity. Conversely, a negative value of sensitivity indicates a decrease in ignition delay time and thus an *increase* in overall reactivity. At high temperatures (1200 and 1500 K) the only primary fuel reactions showing sensitivity are the hydrogen-atom abstractions from the fuel by $\dot{O}H$, $\dot{H}$, and $H\dot{O}_2$ radicals. Other important reactions include $H + O_2 = \ddot{O} + \dot{O}H$ and $\dot{C}H_3 + H\dot{O}_2 = CH_3\dot{O} + \dot{O}H$ which both promote reactivity, while the chain termination reaction $\dot{C}H_3 + H\dot{O}_2 = CH_4 + O_2$ inhibits reactivity.

The reactions with the highest positive sensitivity coefficients (most inhibiting) at 830 K involve the concerted elimination of isobutene and a hydroperoxyl radical from iso- and tert-butylperoxy radicals. These are propagation reactions and thus lead to reduced reactivity and are known to contribute to the NTC behavior of the fuel [23].

$$iC_4H_9\dot{O}_2 = iC_4H_8 + H\dot{O}_2 \quad (1210)$$

$$tC_4H_9\dot{O}_2 = iC_4H_8 + H\dot{O}_2 \quad (1211)$$

In addition, the reaction $H\dot{O}_2 + H\dot{O}_2 = H_2O_2 + O_2$ is strongly inhibiting as it consumes *two* hydroperoxyl radicals, producing just one molecule of hydrogen peroxide. By contrast, we see that both fuel $+H\dot{O}_2$ reactions producing iso- and tert-butyl radicals promote reactivity, as in these reactions *one* hydroperoxyl radical produces one molecule of hydrogen peroxide. Subsequently, hydrogen peroxide decomposes into *two* hydroxyl radicals, a reaction which also promotes reactivity.

Hydrogen atom abstraction from the fuel by hydroxyl radicals shows some interesting behavior. At low temperatures (800 and 950 K), abstraction producing an iso-butyl radical (1021) promotes reactivity, while production of a tert-butyl radical (1020) inhibits reactivity. The situations are the opposite at high temperatures (1200 and 1500 K).

$$iC_4H_{10} + \dot{O}H = t\dot{C}_4H_9 + H_2O \quad (1020)$$

$$iC_4H_{10} + \dot{O}H = i\dot{C}_4H_9 + H_2O \quad (1021)$$

At low temperatures, where the chain-branching mechanism depends upon a series of radical additions to molecular oxygen and inter-molecular hydrogen-atom isomerization reactions, more iso-butyl radicals proceed through this chain-branching mechanism than do tert-butyl radicals. Thus, the following series of reactions promotes reactivity:

$$iC_4H_8OOH - i\dot{O}_2 = iC_4ketii + \dot{O}H \quad (1215)$$

$$iC_4H_9\dot{O}_2 = i\dot{C}_4H_8OOH - i \quad (1207)$$

$$i\dot{C}_4H_8OOH - i + O_2 = iC_4H_8OOH - i\dot{O}_2 \quad (-1212)$$

By contrast, at high temperatures the uni-molecular β-scission of alkyl radicals dominates over the bimolecular addition to molecular oxygen. Decomposition of tert-butyl radicals generates isobutene and a hydrogen atom, which is a reactive radical, while the iso-butyl radical produces propene and methyl, a relatively unreactive radical. Subsequent hydrogen-atom abstraction from both isobutene and propene will produce the resonantly stabilized methyl allyl and allyl radicals, respectively.

The decomposition of iso-butyl to propene and a methyl radical inhibits reactivity at 830 K and shows a decreasing sensitivity at higher temperatures. This behavior is because at lower temperatures the reaction competes with addition to molecular oxygen, and increasing the rate of alkyl radical decomposition reduces the rate of alkyl-peroxy radical formation and subsequent chain-branching reactions.

Fig. 7 depicts sensitivity coefficients as functions of equivalence ratio for isobutane/air mixtures at 950 K and at a pressure of 20 atm. This figure shows higher sensitivity coefficients for rich mixtures when compared to the stoichiometric case. In contrast, lean mixtures show the lowest sensitivity and the very high importance of hydoperoxy- and methylperoxyl-radical chemistry, where the most promoting reaction is: $iC_4H_{10} + H\dot{O}_2 = t\dot{C}_4H_9 + H_2O_2$, which indicates the importance of the hydroperoxyl radical at this temperature (and pressure). The most inhibiting reaction is $H\dot{O}_2 + H\dot{O}_2 = H_2O_2 + O_2$, and the next most inhibiting reaction is $\dot{C}H_3 + H\dot{O}_2 = CH_4 + O_2$. The competing reaction $\dot{C}H_3 + H\dot{O}_2 = CH_3\dot{O} + \dot{O}H$ promotes reactivity.

It is interesting to note the sensitivity to methylperoxyl ($CH_3\dot{O}_2$) radical chemistry. H-atom abstraction from the fuel producing both iso- and tert-butyl radicals promotes reactivity at 950 K. However, this same sensitivity to methylperoxyl-radical chemistry was not seen in our *n*-butane study [5]. For branched alkanes, methyl-radical chemistry is more important than for the straight-chained isomer.

$$iC_4H_{10} + CH_3\dot{O}_2 = i\dot{C}_4H_9 + CH_3O_2H \quad (1032)$$

$$iC_4H_{10} + CH_3\dot{O}_2 = t\dot{C}_4H_9 + CH_3O_2H \quad (1045)$$

Other inhibiting reactions include the molecular elimination of isobutene and hydroperoxyl radicals from iso- and tert-butoxy radicals and also β-scission of iso-butyl radical all discussed above.

A sensitivity analysis to equivalence ratio at 830 and 1200 K was also performed and is provided as Figs. 4 and 5 of the supplemental material. An understanding of the sensitivity coefficients of these figures can be easily derived considering the preceding discussion.

4.5. Comparison with other shock-tube measurements

Oehlschlaeger et al. [10] measured ignition times and $\dot{O}H$ radical concentration time histories behind reflected shock waves during the oxidation of isobutane (and also iso-pentane and iso-octane). Initial reflected-shock conditions ranged from 1177 to 2009 K and 1.10 to 12.58 atm with dilute fuel/O_2/Ar mixtures varying in fuel concentration from 100 ppm to 1.25% by volume and in equivalence ratio from 0.25 to 2. Fig. 8 shows a comparison of the current model together with the experimental data of Oehlschlaeger et al., plotted as solid symbols. Some of the experimental conditions were repeated in the present study, and these results are plotted as open symbols. There is overall very good agreement between the experimental measurements and the model predictions, but there is a trend in that rich mixtures are predicted to be faster than experiment, while ignition delay predictions for lean mixtures are slower than experiment.

Fig. 8a shows the effect of dilution under stoichiometric conditions and at an average reflected-shock pressure of 1.5 atm. As shown, the more concentrated the mixture the faster is the ignition time. In addition, the repeat data of this study at 0.1%, 0.5% and 1.0% isobutane are always slightly slower than those recorded by Oehlschlaeger et al., while the model is in very good agreement with the Oehlschlaeger data. This is not too surprising as ignition times are sensitive to uni-molecular fuel decomposition reactions, and these are taken from the work of Oehlschlaeger et al. [12]. The 0.05% isobutane mixture ignition delay time versus inverse temperature profile has a concave shape (and the 0.01% mixtures profile is slightly convex) for both the experiments and the model. This result is due to variations in pressure for individual points and not to some chemistry effect. In modeling the data, we do not simulate every experimentally measured temperature point, but only representative ones which encapsulate the complete range; but in the simulations we do use the experimentally measured pressure at the chosen temperature. For example, at 1444 and 1546 K the reflected-shock pressure was 1.59 and 1.58 atm, while at 1630 and 1703 K it was 1.49 and 1.40 atm, respectively.

Fig. 8b depicts the influence of pressure for 0.05% isobutane, 3.25% oxygen and 96.25% argon, at average reflected-shock pressures of 1.5, 2.6, 5.0, and 10 atm. Again, as the pressure increases, which is an effective increase in concentration, the ignition delay time becomes faster. The model agreement with the data is excellent with the influence of pressure (and temperature) being accurately reproduced. In addition, the concave shape of the profile particularly at 2.6 atm is again due to a drop in shock pressure to 2.0 atm for the highest-temperature point.

Finally, Fig. 8c shows the influence of equivalence ratio at a constant oxygen concentration of 3.25% and varying the fuel concentration from 1.0% to 0.125% for mixtures diluted in argon at an average reflected-shock pressure of 1.5 atm. As seen in Fig. 8c, a large effect on ignition delay times in which each doubling of the fuel concentration leads to a substantial *increase* in ignition delay times. This trend is consistent with shock-tube studies in which correlations of ignition delay times show a positive dependence on fuel concentration, at least at the higher temperatures. For example, the high-temperature τ_{ign} correlation presented above shows a slightly positive exponent (0.06) for the isobutane concentration (although the reader should be reminded that this correlation was derived for the undiluted fuel–air mixtures explored herein). The model agrees well with the more-dilute data but is slightly slow (about 30%) for the 1.0% isobutane mixture at ϕ = 2.0).

Ogura et al. [11] in 2007 performed shock-tube experiments to measure ignition delay times behind reflected shock waves for *n*-butane, isobutane and mixtures of 50/50 *n*-butane/isobutane. Fig. 9 shows a comparison of the model with the experimental data of Ogura et al. as well as additional data taken in the present study to further validate this set of conditions for a mixture of 50/50 *n*-butane/isobutane with 9% O_2 and 90% argon by volume. A table of the new data points for this mixture is provided in the supplemental material. As seen in Fig. 9, the model is in excellent agreement with the repeat data points, which are also is good agreement with the original data from Ogura et al. [11] at the higher temperatures. Additional discussion concerning the comparison of butane isomer blends is provided in the following section.

5. Comparison of butane isomer mixtures

Figs. 10–12 show both experimental and model results for 100% isobutane, 50/50 *n*-butane/isobutane and 100% *n*-butane mixtures

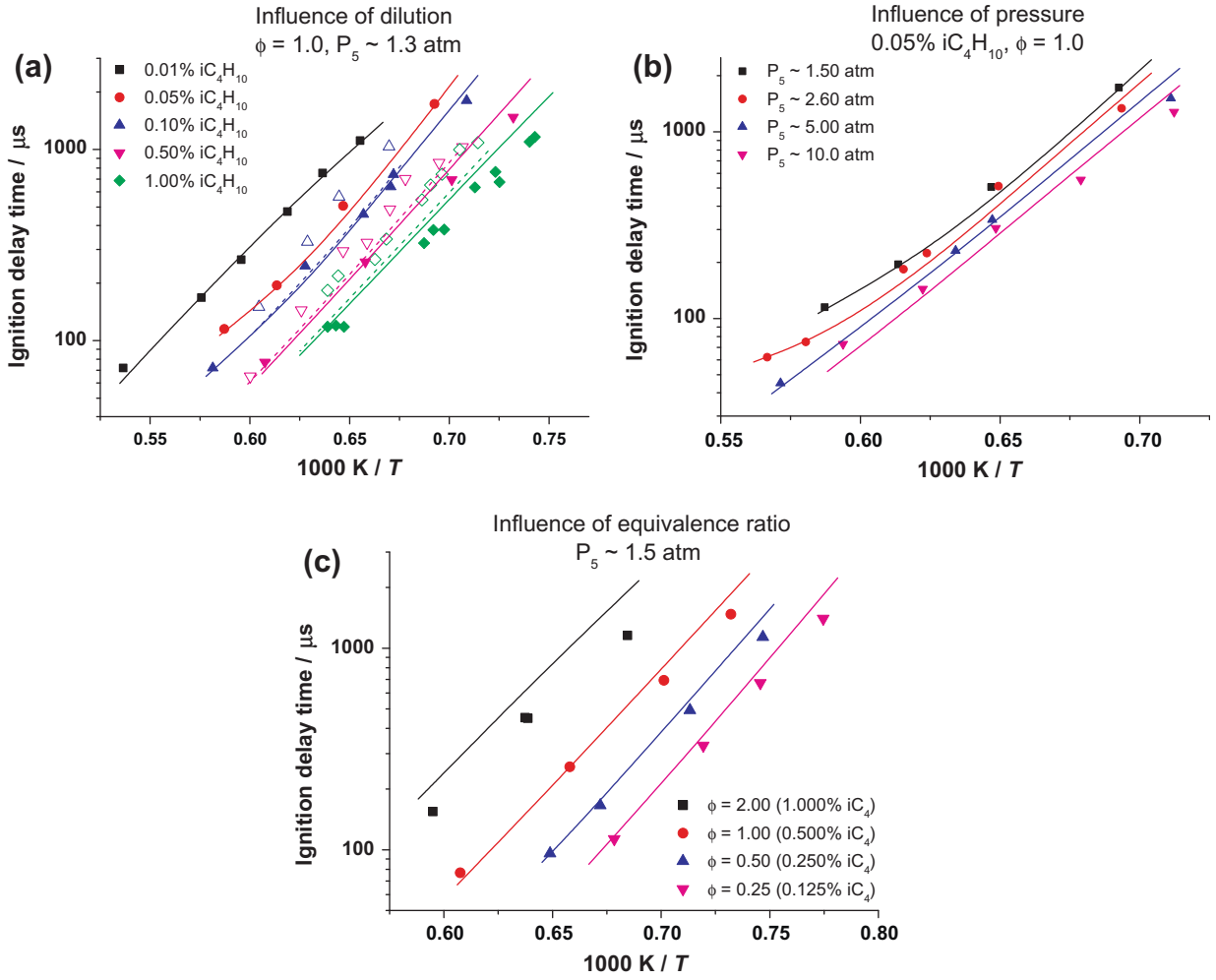

Fig. 8. Comparison of ignition delay times for dilute iso-C_4H_{10} oxidation in Ar, solid points are experimental results from Oehlschlaeger et al. [10], open symbols this study, and lines are model simulations, solid lines correspond to solid symbols while dotted lines correspond to open symbols.

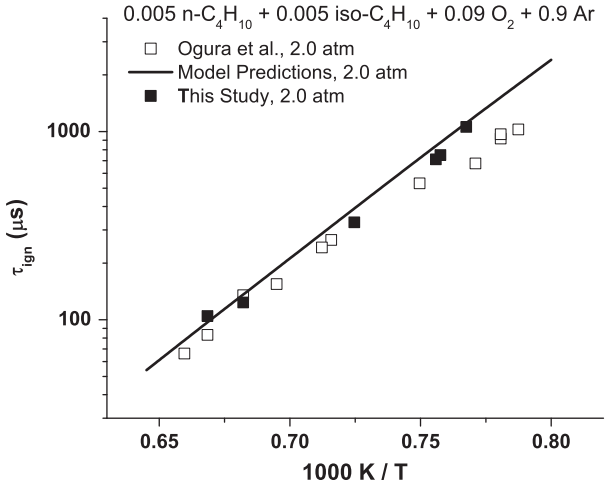

Fig. 9. Experimental shock-tube results performed in this study agree well with the model and with the original data taken by Ogura et al. [11] for the same 50/50 mixture of *n*-/*i*-butane diluted in 90% argon.

at approximately 2 and 20 atm. Other comparisons at 10 atm are included as Figs. 6–8 in the supplemental material. The *n*-butane data are from the companion paper [5], while the 50/50 data are from the recent paper by the authors [4]. In all figures, the isobutane is slowest to ignite, while *n*-butane is fastest, with the 50/50 mixture showing intermediate reactivity between the two. Fig. 10a compares the three mixtures at $\phi = 0.5$ in "air" at an average reflected-shock pressure of 2 atm, where it was only possible to record high-temperature shock-tube data. There is overall excellent agreement between the simulations and the experimental results. For the same mixtures at 20 atm, Fig. 10b, it was possible to record low-temperature RCM data in addition to shock-tube data. At high-temperatures, it is difficult to discern any noticeable difference between the mixtures as the extensive range of study tends to merge the data, but experiment and model do show that isobutane mixtures are slowest to ignite with *n*-butane fastest at closer inspection. At low temperatures, the situation is much clearer with isobutane ignition times measured to be significantly longer than those for *n*-butane, particularly in the temperature range 660–900 K. For isobutane, in the temperature range 770–900 K, the model considerably over-predicts ignition times.

Similar results are shown in Fig. 11a and b for stoichiometric mixtures. For the isobutane isomer at high-temperature and 1-atm pressure, the model is in poor agreement. Notwithstanding some scatter in the experimental data at this pressure, it appears that some improvement can still be made in the mechanism under these conditions. At 20 atm, Fig. 11b, the model is in reasonably good agreement with all data.

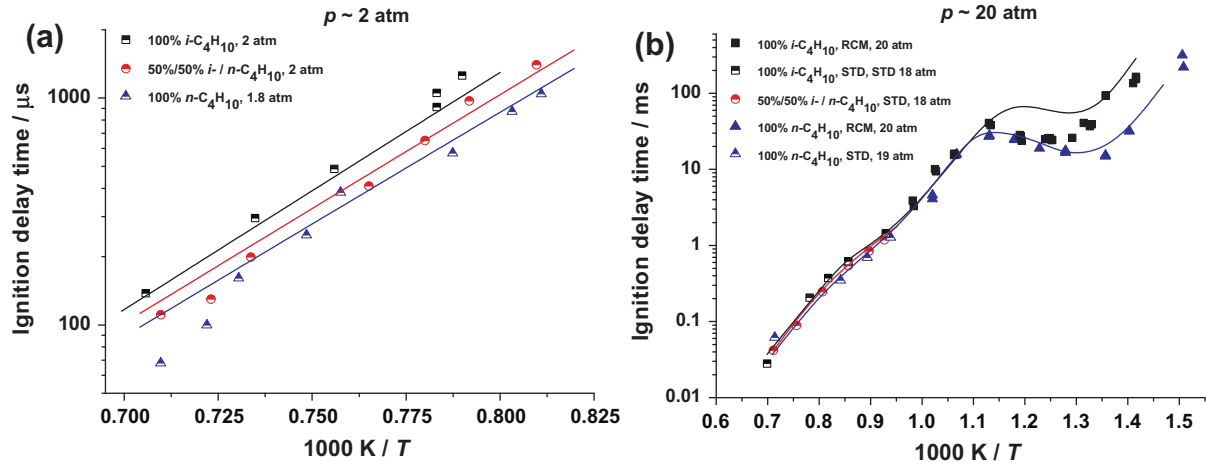

Fig. 10. Comparison of ignition delay times for isobutane, 50/50 *n*-/isobutane [4], and *n*-butane [5] mixtures in "air" at $\phi = 0.5$, (a) $p \approx 2$ atm and (b) $p \approx 20$ atm. Lines are model simulations.

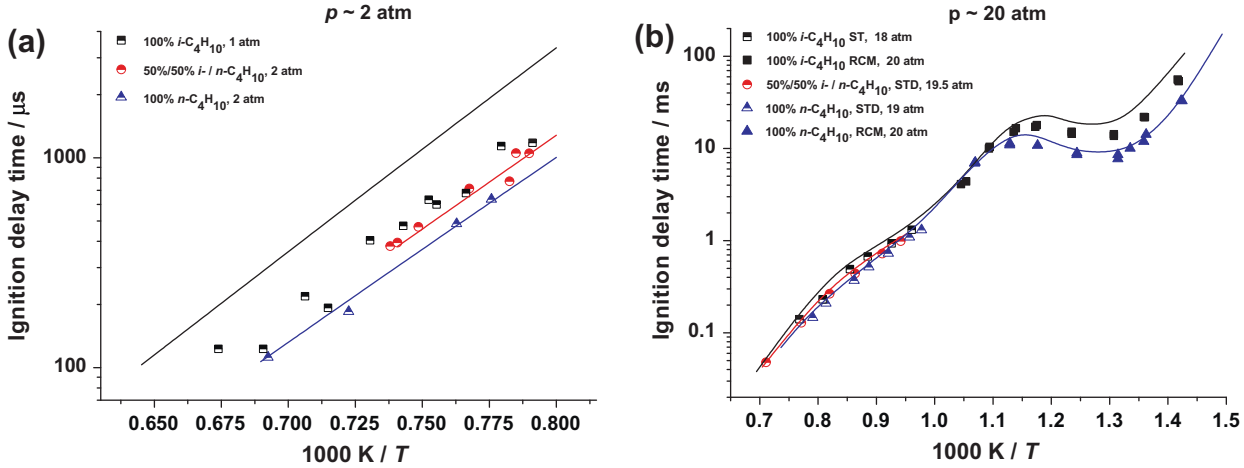

Fig. 11. Comparison of ignition delay times for isobutane, 50/50 *n*-/isobutane [4], and *n*-butane [5] mixtures in "air" at $\phi = 1.0$, (a) $p \approx 2$ atm and (b) $p \approx 20$ atm. Lines are model simulations.

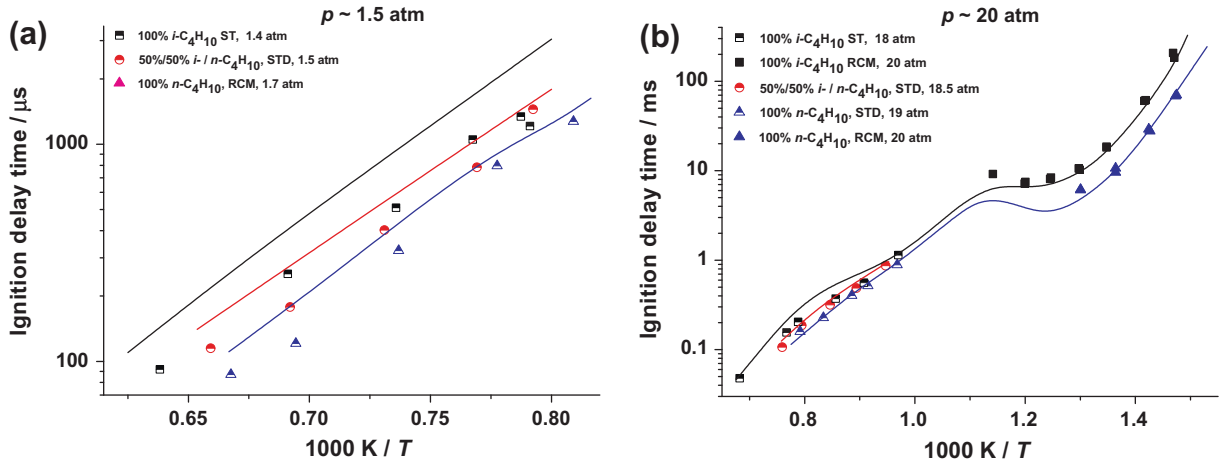

Fig. 12. Comparison of ignition delay times for isobutane, 50/50 *n*-/isobutane, and *n*-butane mixtures in "air" at $\phi = 2.0$, (a) $p \approx 1.5$ atm and (b) $p \approx 20$ atm. Lines are model simulations.

For rich mixtures ($\phi = 2$), Fig. 12a and b, again there is relatively poor agreement between model and experiment at low pressure and high temperature. However, at 20 atm, the model reproduces the data very well. The strange concave shape of the data and

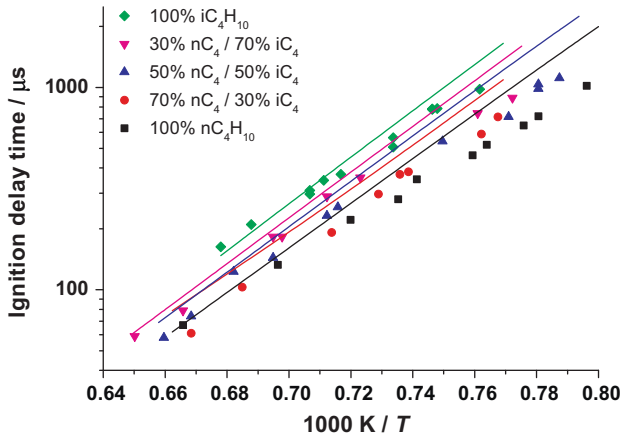

Fig. 13. Comparison of model simulations (lines) versus experimental (points) [11] ignition delay times for 1.0% C_4H_{10}, 9.0% O_2, 90% Ar mixtures at $p \approx 2.0$ atm.

model simulation for isobutane at high temperature is due to a lower measured pressure (14 atm) at 1250 K compared to the average of 18-atm average pressure listed in the plot.

Fig. 13 compares model predictions with the experimental results of Ogura et al. [11] for pure *n*-butane and isobutane fuels and their mixtures at 1.0% fuel, at $\phi = 0.72$ diluted in argon at a pressure of approximately 2 atm. It was found that pure isobutane was slowest to ignite and *n*-butane the fastest, with ignition times in the order 100% *i*-C_4 > 70% *i*-C_4/30% *n*-C_4 > 50% *i*-C_4/50% *n*-C_4 > 30% *i*-C_4/70% *n*-C_4 > 100% *n*-C_4. This trend is reproduced by the model. However, at lower temperatures the model is slower than the experimental measurements for both the pure components and their mixtures with the predicted activation energy being higher than that measured experimentally.

Further examination of predicted mechanism ignition times for the various butane isomer blends reveals a significant dependence on stoichiometry. Since the model has been shown in this paper to predict the experimental data very well, it can be used to perform parametric studies to examine blends between the ranges of 100% *n*-butane and 100% isobutane. Fig. 14 compares model-calculated ignition delay times obtained for a mixture of 100% *n*-butane through to a mixture of 100% isobutane by varying blends of the two isomers in between the two extremes, all at higher temperatures and a pressure of 1 atm. Each plot represents an extreme in stoichiometry, i.e., $\phi = 0.3$ and $\phi = 2.0$. At fuel-lean conditions, Fig. 14a, 100% *n*-butane and 100% isobutane are shown to have similar ignition times, although the isobutane ignition times are slightly larger. However, the model calculations show that the difference between the two isomers becomes more pronounced as the fuel–air mixture becomes more fuel rich. For example, the difference in ignition time between the two isomers becomes quite larger at $\phi = 2.0$, as seen in Fig. 14b.

Furthermore, higher pressure also diminishes the differences in ignition times between butane isomers, particularly at higher temperatures. Fig. 15 compares model results for the same stoichiometry ($\phi = 1.0$), but for two different pressures (1 atm, 18 atm). At the higher pressure, the differences in ignition delay time between the two fuels at higher temperatures become almost insignificant.

6. Conclusions

High-pressure experiments were performed using both the shock-tube and the rapid compression machine techniques, resulting in the most thorough set of isobutane ignition delay times currently available. Equivalence ratios for the undiluted fuel–air experiments included values of 0.3, 0.5, 1, and 2; the measured pressures were approximately 1, 10, 20, and 30 atm; and the temperatures ranged from 590 to 1567 K. Excellent agreement was seen between the RCM and ST data sets, where at the intermediate temperature ranges the ignition data from the two facilities link up nicely for common equivalence ratios and pressures. It was found that these data also agree quite well with others available in the literature, namely those recorded by Griffiths et al. [8] at 10 atm, but were generally slower than those recorded by Gersen et al. in an RCM at 15 and 30 atm. Other conditions from the literature were repeated herein with mostly good agreement for the dilute-mixture data of Oehlschlaeger et al. [10] and Ogura et al. [11]. Empirical correlations of the higher-temperature data were also determined.

Central to the work herein was the construction and validation of a detailed chemical kinetic model consisting of 230 species and 1328 reactions. This model has been built up over the past few years using validation data from high-pressure, undiluted fuel–air ignition experiments, among others, involving hydrocarbon compounds with carbon content ranging from C_1 to C_4. It was shown in this paper that the model displays remarkable agreement with the experimental data, especially when one considers the

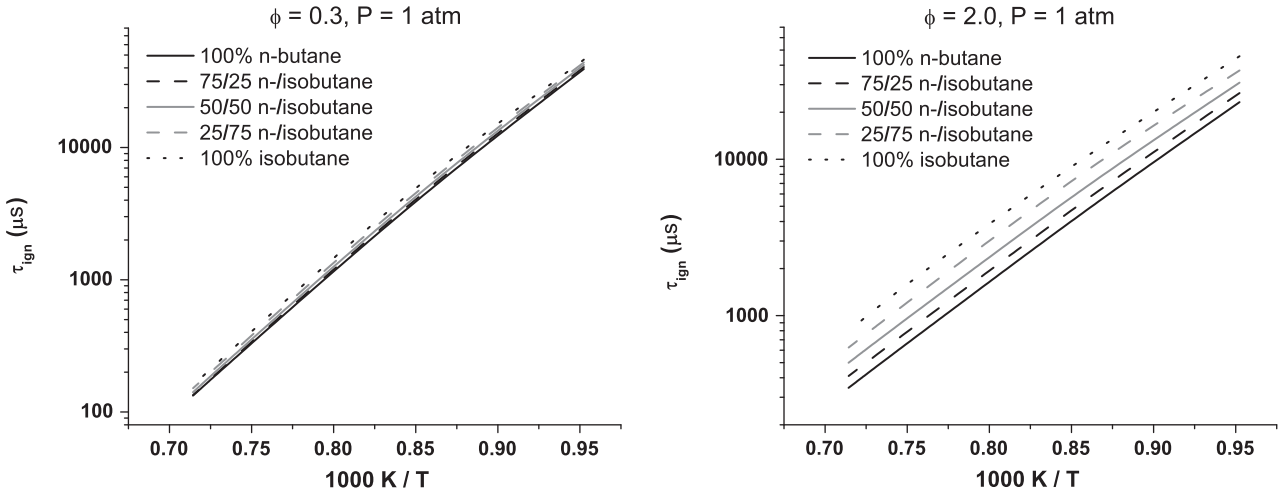

Fig. 14. Model-simulated effect of equivalence ratio on the ignition delay times of isomer blends at higher temperatures. Calculated ignition delay times for various fuel blends at 1 atm show *n*-butane to be more readily ignitable than isobutane at richer conditions. At fuel-lean conditions ($\phi = 0.3$), the difference in butane isomers becomes less distinct.

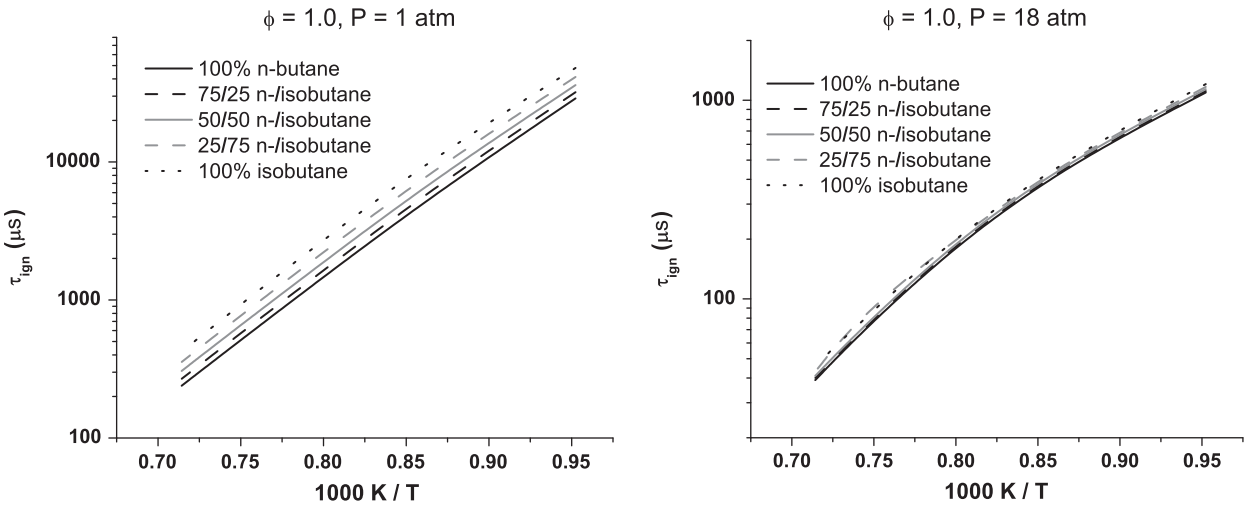

Fig. 15. Calculated effect of pressure on isomer-blend composition at higher temperatures. The model-simulated ignition delay times at stoichiometric conditions show a greater distinction between butane isomers at low-pressure (1 atm) than at elevated pressure (18 atm).

wide range of conditions and kinetic channels involved, including high- and low-temperature chemistry, high- and low-pressure kinetics, and NTC behavior. The model was used to perform reaction pathway and ignition delay time sensitivity analyses for conditions representative of the present work. It was found that one of the most important reactions inhibiting reactivity is the concerted elimination reaction: $\mathrm{i-,t-C_4H_9\dot{O}_2 = iC_4H_8 + H\dot{O}_2}$. Despite the comprehensiveness and accuracy of the detailed mechanism displayed thus far, some improvements can still be made, particularly for stoichiometric and rich mixtures at lower temperatures and for ignition at pressures near 1 atm. In particular, a detailed analysis of iso-butyl and tert-butyl radical addition to molecular oxygen is warranted with the rate constants for molecular elimination of isobutene and hydroperoxyl radical of great importance. Moreover, we recommend an analysis of hydroperoxy-butyl radical addition to molecular oxygen with a detailed description of the products produced together with rate constant expressions.

Acknowledgments

This work was supported primarily by Rolls-Royce Canada Ltd. Partial support for the experiments came from The National Science Foundation under Grant CBET-0832561 and The Aerospace Corporation. The authors (TAMU) gratefully acknowledge the assistance of Nolan Polley, Madeleine Kopp, Sean Baker, and Daniel Pastrich in performing some of the shock-tube experiments.

Appendix A. Supplementary material

Supplementary data associated with this article can be found, in the online version, at doi:10.1016/j.combustflame.2010.01.011.

References

[1] R.M. Flores, V.G. McDonell, G.S. Samuelson, J. Eng. Gas Turb. Power 125 (2003) 701–708.
[2] M. Moliere, ASME Paper No. GT-2002-30017, 2002.
[3] T. Lieuwen, V. McDonell, E. Petersen, D. Santavicca, J. Eng. Gas Turb. Power 130 (2008). 11506-1-10.
[4] N. Donato, C. Aul, E. Petersen, C. Zinner, D. Healy, H. Curran, G. Bourque, J. Eng. Gas Turb. Power, in press.
[5] D. Healy, H.J. Curran, N.D. Donato, C.J. Aul, E.L. Petersen, C.M. Zinner, G. Bourque, Combust. Flame 157 (2010) 1526–1539.
[6] S. Addagarla, Y. Henig, R.D. Wilk, D.L. Miller, N.P. Cernansky, Society of Automotive Engineers Publication, SAE-892082, 1989.
[7] R.D. Wilk, W.J. Pitz, C.K. Westbrook, S. Addagarla, D.L. Miller, N.P. Cernansky, R.M. Green, Proc. Combust. Inst. 23 (1990) 1047–1053.
[8] J.F. Griffiths, P.A. Halford-Maw, D.J. Rose, Combust. Flame 95 (1993) 291–306.
[9] S. Wang, D.L. Miller, N.P. Cernansky, Society of Automotive Engineers Publication, SAE–962106, 1986.
[10] M.A. Oehlschlaeger, D.F. Davidson, J.T. Herbon, R.K. Hanson, Int. J. Chem. Kinet. 36 (2004) 67–78;
M.A. Oehlschlaeger, D.F. Davidson, J.T. Herbon, R.K. Hanson, AIAA Paper 2003-0830, 41st AIAA Aerospace Sciences Meeting and Exhibit Reno NV, 2003.
[11] T. Ogura, Y. Nagumo, A. Miyoshi, M. Koshi, Energy Fuels 21 (2007) 130–135.
[12] M.A. Oehlschlaeger, D.F. Davidson, R.K. Hanson, J. Phys. Chem. A 108 (2004) 4247–4253.
[13] R.G. Gilbert, K. Luther, J. Troe, Ber. Bunsenges. Phys. Chem. 87 (1983) 169–177.
[14] L. Brett, Ph.D. Thesis, National University of Ireland, Galway, 1999.
[15] L. Brett, J. MacNamara, P. Musch, J.M. Simmie, Combust. Flame 124 (2001) 326–329.
[16] S. Gallagher, H.J. Curran, W.K. Metcalfe, D. Healy, J.M. Simmie, G. Bourque, Combust. Flame 153 (2008) 316–333.
[17] E.L. Petersen, D.M. Kalitan, S. Simmons, G. Bourque, H.J. Curran, J.M. Simmie, Proc. Combust. Inst. 31 (2007) 447–454.
[18] E.L. Petersen, M.J.A. Rickard, M.W. Crofton, E.D. Abbey, M.J. Traum, D.M. Kalitan, Measure. Sci. Technol. 16 (2005) 1716–1729.
[19] D. Healy, H.J. Curran, S. Dooley, J.M. Simmie, D.M. Kalitan, E.L. Petersen, G. Bourque, Combust. Flame 155 (2008) 451–461.
[20] J. de Vries, C. Aul, A. Barrett, D. Lambe, E. Petersen, in: K. Hannemann, F. Seiler (Eds.), Shock Waves: 26th International Symposium on Shock Waves, vol. 1, 2009, pp. 171–176.
[21] H.J. Curran, Int. J. Chem. Kinet. 38 (2006) 250–275.
[22] D.M. Matheu, W.H. Green Jr., J.M. Grenda, Int. J. Chem. Kinet. 35 (2003) 95–119.
[23] J.D. DeSain, S.J. Klippenstein, J.A. Miller, C.A. Taatjes, J. Phys. Chem. A 107 (2003) 4415–4427.
[24] S. Gersen, A.V. Mokhov, J.H. Darmeveil, H.B. Levinsky, Combust. Flame 157 (2010) 240–245.
[25] D.J.M. Ray, R.R. Diaz, D.J. Waddington, Proc. Combust. Inst. 14 (1973) 259–266.
[26] D.J.M. Ray, D.J. Waddington, Combust. Flame 20 (1973) 327–334.